Prediction of Power Amplifier Intermodulation Distortion Behavior

Christian Fager and Herbert Zirath
Microwave Electronics Lab., Dept. of Microtechnology and Nanoscience
Chalmers University of Technology, 412 96 Göteborg, Sweden

***Abstract*— This paper presents an analytical large signal intermodulation distortion (IMD) analysis which allows the origins of IMD in power amplifiers (PAs) to be understood, and the behavior in different classes of operation to be predicted versus input power. Two tone measurements on a 950 MHz RF CMOS PA in different classes of operation are used to illustrate typical behavior and demonstrate application of the method presented.**

I. Introduction

Complex modulation schemes are used in modern wireless communications systems to fulfill the requirements for high data transmission capacity over a minimal frequency spectrum. This implies that the radio transmitters must be made very linear to avoid distortion of the data. Understanding and minimization of intermodulation distortion (IMD) in power amplifiers (PAs) is therefore of great concern in maximizing the overall system performance [1], [2].

The power amplifiers (PAs) are preferably driven with a large signal excursion and biased close to turn on to fulfill the requirements for high output power and efficiency. The signals can therefore not be considered as small deviations from a fixed quiescent point and a true large signal analysis must be performed. Yet, extrapolated small signal IMD measures such as third-order intercept point (IP3) are commonly used to characterize PA IMD [3].

As opposed to small signal operation, no practical algebraic methods exist for prediction of IMD under large signal operating conditions. Numerical methods such as harmonic balance or transient analysis are therefore commonly used. However, the results of such simulations reveal little information about the mechanisms responsible for the behavior obtained.

To better understand the mechanisms responsible for large signal IMD in PAs we here present an approximate, algebraic large signal analysis method.

The operating frequency is throughout the paper assumed sufficiently low for reactive effects to be negligible.

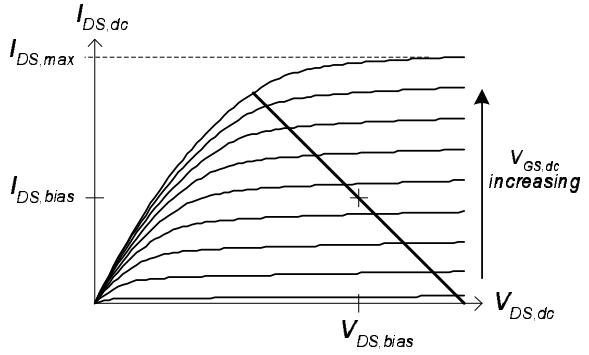

Fig. 1. Typical FET dc I_{DS}/V_{DS} characteristics (thin lines) and load line (thick line) for power amplifier operation.

II. Transfer function representation

For a fixed drain bias voltage (V_{DS}) and load impedance the drain current (i_{DS}) follows a dynamic trajectory which can be plotted together with the transistor I_{DS}/V_{DS} dc characteristics. If reactive effects are neglected, the dynamic trajectory appears as a line, which is normally denoted the *load line*. Fig. 1 shows a load line typically present in PAs.

The load line determines a direct relationship between the input voltage, v_{GS}, and the output current, i_{DS}. The PA may therefore be represented by a nonlinear transfer function (TF).

Fig. 2 shows a typical TF ($i_{DS}\,[v_{GS}]$) obtained in a FET PA. The TF has in this case been determined from harmonic balance simulation with a nonlinear CMOS transistor model, but could also be determined experimentally [4].

For low v_{GS}, the TF essentially follows the I_{DS}/V_{GS} characteristics measured under constant V_{DS} conditions in the saturated region. For higher v_{GS}, the TF compresses as v_{DS} is reduced along the load line. Eventually the TF saturates as the load line reaches the linear-to-saturated region of the FET characteristics (see Fig. 1).

The TF may be used for a behavioral small signal IMD analysis by expanding it in a low order Taylor series,

$$i_{DS}(V_{GS,bias}+v_{gs}) = I_{DS,bias} + G_1 v_{gs} + G_2 v_{gs}^2 + G_3 v_{gs}^3 + \cdots \quad (1)$$

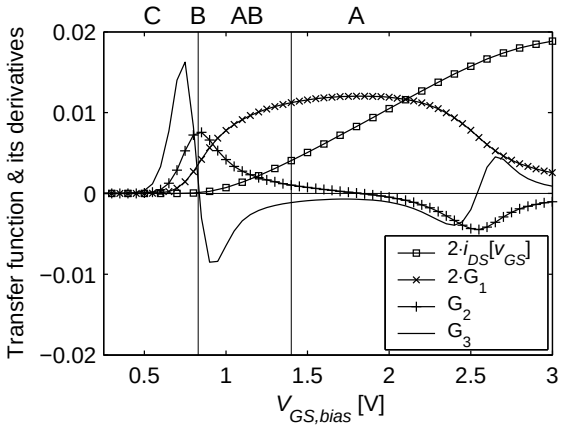

Fig. 2. Typical transfer function and its derivatives obtained versus gate bias voltage ($V_{GS,bias}$) in a FET power amplifier. The corresponding classes of operation are indicated in top of the figure.

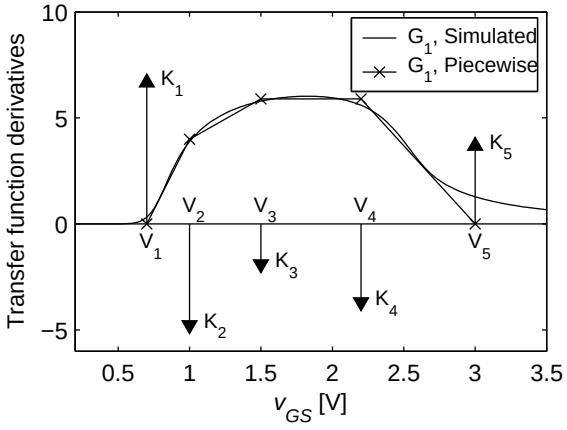

Fig. 3. Piecewise linear approximation of the G_1 versus v_{GS} characteristics. The resulting G_3 becomes a set of Dirac-delta functions as indicated by arrows.

where G_n represent the TF derivatives. The first three derivatives are shown in Fig. 2. The third order TF derivative (G_3) is of particular interest in PA applications as it determines the in-band third order IMD (IM3) [5]:

$$\mathrm{IM3} \propto G_3 A^3 \tag{2}$$

where A is the v_{IN} amplitude. This relationship results in the well-known small signal 3 dB/dB slope of IMD versus input power.

III. Large signal IMD analysis

The bias points of zero G_3 in Fig. 2 are useful for achieving good small signal IMD performance. However, for practical PAs, higher order terms in that were neglected in the small signal analysis become dominant. Their total contribution can however be expressed as a residual term by [6],

$$i_{DS}(V_{GS}+v_{gs}) = i_{DS}(V_{GS}) + G_1 v_{gs} + G_2 v_{gs}^2 + \frac{1}{2}\int_0^{v_{gs}} (v_{gs}-x)^2 G_3(x+V_{GS})dx \tag{3}$$

where v_{gs} is an arbitrary deviation from the bias point, $V_{GS,bias}$.

The G_1 characteristic of Fig. 2 is now approximated by a piecewise linear function to allow for analytical calculations (see Fig. 3). The resulting G_3 becomes a set of Dirac-delta functions (impulses) centered at the breakpoints of the G_1 breakpoints, with magnitudes equal to the change of slope in each of those. The impulses therefore represent, in condensed form, the dominant device and amplifier mechanisms such as device turn on, quadratic-to-linear transitions, and saturation as the load line reaches the linear region.

As a further simplifying assumption, a single sinusoidal input signal is considered,

$$v_{gs}(t) = A\cos\omega t \tag{4}$$

The third harmonic distortion (HD3) is then closely related to the large signal in-band IMD that would appear in e.g. a two tone test.

It is noted that only the last term of (3) can contribute to odd order IMD in i_{ds},

$$i_{DS,3}(t) = \frac{1}{2}\int_0^{A\cos\omega t} (A\cos\omega t - x)^2 \sum_{i=1}^{N} K_i \delta(x+V_{GS}-V_i)\,dx \tag{5}$$

The HD3 in i_{DS} ($I_{ds,3}$) can then be expressed as the third Fourier series coefficient of $i_{DS,3}(t)$,

$$I_{ds,3} = \frac{1}{2\pi}\sum_{i\in\Omega} K_i \int_{-\varphi_i}^{\varphi_i} (A\cos\theta + V_{GS} - V_i)^2 \cos 3\theta\, d\theta \tag{6}$$

with Ω representing the set of impulses being traversed by the input signal. φ_i is the phase for which the input signal reaches the i'th impulse and is given by

$$\varphi_i = \arccos\left(\frac{V_i - V_{GS}}{A}\right) \tag{7}$$

Equation (7) can be used in (6) to yield the following compact expression for $I_{ds,3}$, i.e. HD3:

$$I_{ds,3} = \frac{2}{15\pi}\mathrm{Re}\sum_{i=1}^{N} \frac{K_i\left(A^2-(V_i-V_{GS})^2\right)^{5/2}}{A^3} \tag{8}$$

where the real part allows the summation to extend over all impulses in G_3. According to (8), the large signal HD3 behavior is a sum of independent contributions

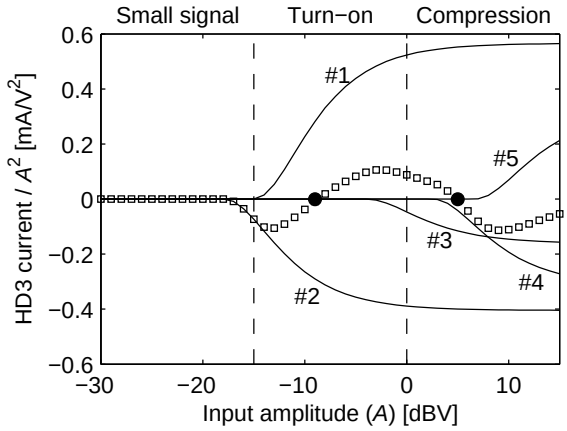

Fig. 4. The total HD3 (markers) and its contributions (lines) predicted by the large signal analysis. The individual contributions are numbered according to the impulses in Fig. 3. The vertical axis is normalized with respect to A^2 to improve plot visibility.

from each of the breakpoints in the piecewise approximation of G_1.

Only a few breakpoints are needed to approximate G_1 well. The mechanisms corresponding each of them may therefore be understood and their individual effect on the large signal IMD behavior be studied versus input power when biased for different classes of operation using (8).

IV. Results

A. Class AB

To exemplify the presented large signal analysis, first class AB operation is considered, where most linear PAs are operated. The piecewise TF in Fig. 3, which was obtained for a CMOS PA, is used.

Each of the TF breakpoints give an individual IMD contribution as soon as it is traversed by the input signal according to the preceding analysis. Fig. 5(a) shows the individual contributions as well as the total HD3 versus input power.

Starting with a negative small signal HD3, originating from the quadratic-to-linear transition (#2) (also observed as a negative G_3 in Fig. 2), the positive turn-on knee contribution (#1) soon starts to dominate and reverses the sign of the total HD3. The negative compression contributions (#3 & #4) again reverse the total HD3 as the input power is further increased, becoming always ultimately negative [5].

Points where the total HD3 is zero (marked with filled circles in Fig. 4) correspond to IMD minima, often denoted large signal sweet spots. These are very beneficial since they can give good IMD performance at high input power levels where efficiency is also good. The behavior in Fig. 4, with double sweet spots is therefore very attractive and understanding its origin important. A similar behavior has been observed in LDMOS transistor PAs [7].

The total HD3 is compared in dB-scale with small signal and harmonic balance analysis results in Fig. 5(a). The large signal analysis is seen to follow the harmonic balance (HB) results very well, even with the small number of impulses used. However, as opposed to the HB results, the large signal analysis can be used to understand what mechanisms are actually cooperating to yield the behavior observed. Adding more impulses will push the validity of the analysis towards lower power levels, but on the other hand prevent identification of the mechanisms corresponding to them.

Fig. 5(b) shows two tone measurement results obtained for a 950 MHz CMOS PA [8] operated in class AB. These results verify that double IMD minima behavior is observed also in practice. The large signal analysis can therefore be used to understand its origin. The IMD versus input power slope is 2.2 dB/dB at low input power, which shows that a traditional small signal analysis is not applicable even for such low input power levels.

B. Class C

The simulation results obtained for class C operation is shown in Fig. 6(a). The device is now biased below turn-on, which makes the positive turn-on contribution (#1) very dominating. Only close to saturation can the negative, compressing, contributions reverse $I_{ds,3}$. This change of sign corresponds to the upper HD3 sweet spot. Also the CMOS PA measurements present this behavior (see Fig. 6(b)), which has also been observed in LDMOS and MESFET PAs [5], [7].

V. Conclusions

An analysis of the large signal IMD behavior of PAs has been presented. As opposed to the numerical methods normally used for large signal IMD prediction, it may be used to understand how fundamental device and PA mechanisms interact in creating the IMD versus input power behavior measured. It could therefore also be used as a tool for optimization of device characteristics with respect to IMD behavior.

Acknowledgement

The authors would like to thank Prof. José Carlos Pedro and Prof. Nuno Borges de Carvalho, Telecommunications Institute, Aveiro, Portugal, and Dr. Fernando Fortes, Telecommunications Institute, Lisbon, Portugal, for sharing their amplifier and measurement data.

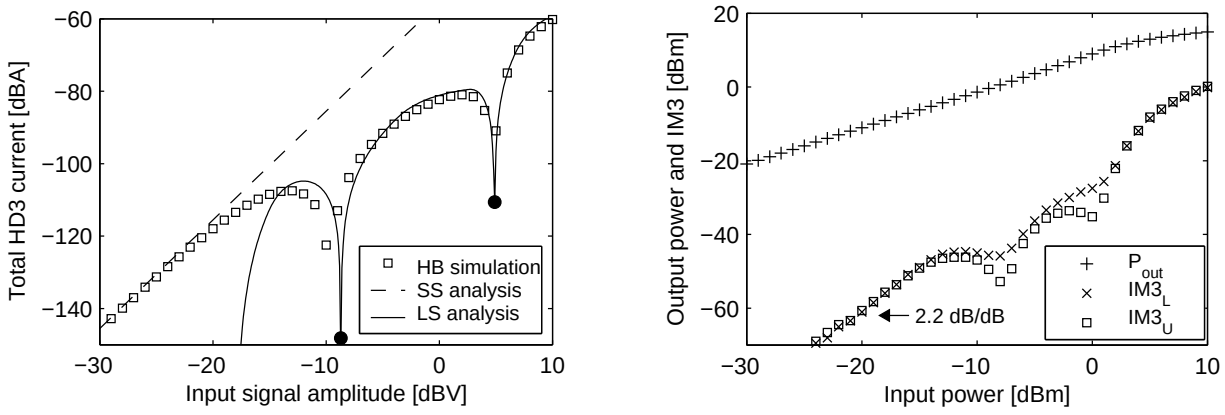

(a) (b)

Fig. 5. (a) Class AB HD3 predicted with small signal (SS), large signal (LS), and harmonic balance (HB) simulations. (b) Measured class AB two tone output power (P_{out}) and upper/lower IMD ($\mathrm{IMD_U}$/$\mathrm{IMD_L}$). The low power IMD slope is indicated.

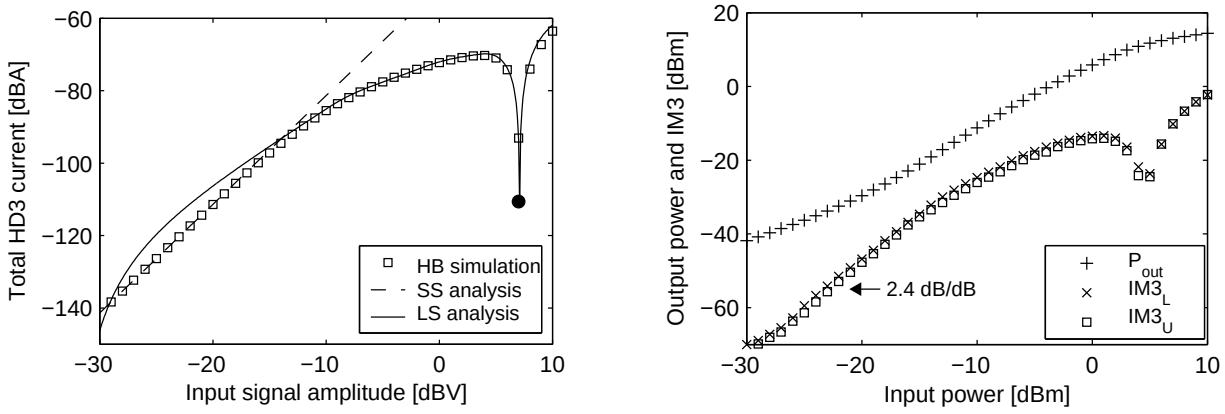

(a) (b)

Fig. 6. (a) Class AB HD3 predicted with small signal (SS), large signal (LS), and harmonic balance (HB) simulations. (b) Measured class C two tone output power (P_{out}) and upper/lower IMD ($\mathrm{IMD_U}$/$\mathrm{IMD_L}$).

REFERENCES

[1] E. Costa, M. Midrio, and S. Pupolin, "Impact of amplifier nonlinearities on OFDM transmission system performance," *IEEE Communications Lett.*, vol. 3, no. Feb., pp. 37–9, 1999.

[2] S. C. Cripps, *RF power amplifiers for wireless communications*, ser. Artech House microwave library. Boston: Artech House, 1999.

[3] S. Maas, *Nonlinear microwave circuits*. Piscataway: IEEE Press, 1997.

[4] C. Fager, "Microwave FET modeling and applications," Ph.D. Thesis, Chalmers University of Technology, 2003.

[5] N. Carvalho and J. Pedro, "Large- and small-signal IMD behavior of microwave power amplifiers," *IEEE Trans. Microwave Theory Tech.*, vol. 47, no. 12, pp. 2364–74, Dec. 1999.

[6] L. Råde and B. Westergren, *Beta : Mathematics handbook*. Bromley: Chartwell-Bratt, 1990.

[7] C. Fager, J. Pedro, N. Carvalho, and H. Zirath, "Prediction of IMD in LDMOS transistor amplifiers using a new large-signal model," *IEEE Transactions on Microwave Theory and Techniques*, vol. 50, no. 12, pp. 2834–42, Dec. 2002.

[8] F. Fortes and M. J. Rosário, "A second harmonic class F power amplifier in standard CMOS technology," *IEEE Trans. Microwave Theory Tech.*, vol. 49, no. 6, pp. 1216–20, June 2001.